Electronic and structural properties of diamond (001) surfaces terminated by selected transition metals

Amit K. Tiwari, J. P. Goss, P. R. Briddon, Nick G. Wright, and Alton B. Horsfall
School of Electrical and Electronic Engineering, Newcastle University, Newcastle upon Tyne, NE1 7RU, United Kingdom

M. J. Rayson
Department of Engineering Sciences and Mathematics, Luleå University of Technology, Luleå S-97187, Sweden
(Received 11 June 2012; revised manuscript received 10 September 2012; published 1 October 2012)

The presence of adsorbate species on diamond surfaces, even in small concentrations, strongly influences electrical, chemical, and structural properties. Despite the technological significance, coverage of diamond by transition metals has received relatively little attention. In this paper, we present the results of density functional calculations examining up to a monolayer of selected metals (Cu, Ni, Ti, and V) on the (001) diamond surface. We find that addition of carbide forming species (Ti and V) results in significantly higher adsorption energies at all surface coverages relative to those of the non-carbide-forming species. For monolayer coverage by Cu or Ni, and submonolayer coverage by Ti and V, we find large, negative electron affinities. We propose that based upon the electron affinities and binding energies, metal-terminated (001) diamond surfaces are promising candidates for electron emission device applications.

DOI: 10.1103/PhysRevB.86.155301 PACS number(s): 73.30.+y, 73.20.At, 68.47.Fg, 68.43.Bc

I. INTRODUCTION

Owing to the superlative material properties of diamond in conjunction with the excellent adhesion and electrical characteristic of transition metals (TMs), TM-diamond interfaces are obvious candidates for solid-state devices operating under extreme conditions.[1–7] Research conducted on TM-coated diamond surfaces suggests that a significant reduction in electron affinity is achievable,[8–13] facilitating the use of diamond for cold cathode electron emission applications,[14,15] including the realization of thermotunnel devices.[16]

To fully understand the characteristics of TM-diamond interfaces, detailed knowledge of the electronic and structural properties is necessary, for which quantum-chemical simulations are well placed to provide both qualitative and quantitative data. Previously, investigation of metal-semiconductor interfaces has largely been of wide-gap, ionic semiconductors and covalent narrow-gap semiconductors.[8,17–20] Diamond, as a wide-gap, covalently bonded material, has received relatively little theoretical attention to date.

Surface electron affinity (EA) is a key characteristic of TM-diamond interfacial characteristics relevant to electronic devices. TM-semiconductor interfaces for Si and Ge, as well as some group III–V compounds, use a number of models to extract an electron-emission barrier height, ϕ_B, from the EA.[17,21,22] According to the most commonly used Schottky-Mott model for an ideal interface between a metal and a p-type semiconductor used[10,11] for metal-diamond interfaces, the barrier height can be described as a function of EA as

$$\phi_{\mathrm{B}} = E_{\mathrm{G}} - (\phi_{\mathrm{M}} - \chi), \tag{1}$$

where ϕ_{M} is the metal work function, χ the EA, and E_{G} the diamond band gap. The EA is by how much energy the vacuum level lies above the conduction-band minimum, and may be either positive (PEA) or negative (NEA). For diamond, it has been shown that the sign of the EA can be engineered by a careful control over the surface termination,[23–26] which in turn provides some control over the characteristics for device applications. Hydrogen-terminated diamond surfaces exhibit an NEA, where theoretically[23,24] and experimentally,[25] the conduction-band minimum lies in the range of 1–2 eV above the vacuum level. A large NEA enables conduction-band electrons to be emitted into vacuum with little or no barrier. In contrast, a PEA, such as determined for carbon, oxygen, or halogen termination,[23–25] increases the barrier height.

Diamond with an NEA is of particular interest for thermionic applications because of the underlying electrical and thermal properties intrinsic to diamond.[27] Although H termination yields a large NEA, it is far from ideal, as the subsequent work function (∼3.6 eV) is high. Furthermore, high-temperature operation (above ∼700 °C) results in desorption of the terminating species, and the resulting hydrogen-deficient surface has a PEA,[11,25] further increasing the work function. Termination by caesium or caesium oxide, which also results in a NEA, also degrades[28,29] at elevated temperatures (above ∼400 °C). Polar, thermally stable options therefore remain to be found for high-temperature thermionic applications.

Recently, ultrathin (a few Å) coatings of TMs on diamond have been considered for thermally stable NEA structures. Experimental evidence for an NEA with Cu, Ni, Co, Zr, Au, and Ti, suggests that such surface treatments may be promising candidates for thermally stable surfaces with low potential barrier heights, even at monolayer (ML) coverage.[10–13] For example, submonolayer deposition of titanium on diamond (111) surfaces yield[13] an NEA and a Schottky barrier height of 1 ± 0.20 eV.

Quantum chemical calculations[30–32] for TM-diamond interfaces have demonstrated that, in addition to the chemical nature of TMs, surface coverage has a discernible effect upon adhesion and electronic properties. For example, Ti adatom and 25% surface coverages exhibit significantly different adsorption energies of 7.19 and 6.62 eV, respectively.[30] Although results of a recent study on Cu- and Ti-diamond (111)-oriented interfaces are not directly comparable to the

present study, the calculated work of separation, which is the measure of interfacial adhesion, decreases with the carbide formation enthalpy ΔH_f (Ti < Cu),[32] (i.e., more energy is required to remove a carbide forming metal from the diamond surface). Schottky barrier heights of TM-diamond interfaces have been examined both in computational and experimental studies,[10–13,31] but the impact of ultrathin metal layers on the stability and electrical/electronic properties is largely unexplored at an atomistic level. To understand the complex interactions between metals and the diamond surface, quantum-mechanically based computational studies are of great interest. In this paper, we present the results of density functional simulations of diamond (001) surfaces covered by up to a monolayer by Cu, Ni, Ti, and V, the choice of metals guided in part by the metals used in experiment, and in part to include metal species which have qualitatively different carbon chemistries.

II. METHOD

Local-density-functional calculations,[33] using the AIMPRO code,[34,35] have been performed. Atoms are modeled using norm-conserving, separable pseudopotentials,[36] and the Kohn-Sham eigenfunctions are expanded using atom-centered Gaussian basis sets.[37] The basis consist of independent sets of s-, p-, and d-type Cartesian Gaussian functions of four widths, amounting to forty functions per atom. Additionally, sets of a combination of sixteen s- and p-Gaussian basis functions are placed at points in the vacuum region with an equal density to the atomic density of the diamond host. This is required to allow for the evanescent decay of electronic states at the surface.[23] Matrix elements of the Hamiltonian are determined using a plane-wave expansion of the density and Kohn-Sham potential[38] with a cutoff of 175 Ha, resulting in convergence of the total energy with respect to the expansion of the charge density to within around 10 meV.

Structures are optimized using a conjugate gradients scheme, with the optimized structures having forces on atoms of $<10^{-3}$ atomic units, and the final structural optimization step is required to result in a reduction in the total energy of less than 10^{-5} Ha.

For bulk diamond, our computational approach yields an equilibrium lattice parameter of 3.53 Å, just 1% less than experiment.[39] The calculated indirect band gap of bulk diamond is 4.20 eV, reflecting the well-documented underestimate of the band gap arising from the underpinning methodology, and is consistent with previous calculations.[40] Surfaces are modeled in a slab geometry, using a periodic boundary condition with equal termination on both surfaces, 14 layers of carbon atoms, and a minimum of 13 Å of vacuum. The slab used is adequately thick to closely represent the bulk material and gives well-converged total energies. Surfaces are modeled using cells with in-plane lattice vectors made up from $n[110]a_0/2$ and $m[1\bar{1}0]a_0/2$, n and m being integers. The calculated lattice constants for ground-state configurations of Cu (3.54 Å), Ni (3.42 Å), Ti ($a = 2.87$, $c = 4.55$ Å), and V (2.91 Å) are with 4% of experiment, and within around 1% of previous comparable calculations.[41,42] The heat of formation for TiC and VC are reproduced to 1% of experiment.[43,44] Work functions for bulk metals (Cu:4.76, Ni:5.23, Ti:4.36, and V:4.34 eV) are calculated to within 0.1 eV of literature values.[45] Based upon these comparators, we conclude that the treatment of the TMs is within the norm of LDA calculations, and suitable for the current study.

For surfaces with submonolayer coverages, a wide variety of symmetrically nonequivalent structures were explored to establish the most probable candidate for the lowest-energy arrangement. For example, with 25% coverage, surface cells with (2×2) and (4×1) arrangement, along with the permutations of arrangements with (4×2), (4×4), and (8×1) periodicities were included. It is worth noting here that the metal-carbon bond lengths vary significantly. In this manuscript, we have included only those relaxed structures for which the bond lengths are within 15% of the reported metal-carbon bond lengths in the corresponding organometallic compounds.[46]

In all cases the Brillouin zone is sampled using uniform Monkhorst-Pack sampling meshes.[47] For surface calculations the Brillouin zone is two dimensional. The sampling used is 8×8 for $n = m = 1$, which is sufficiently dense to achieve an absolute energy convergence better than 10 meV. For simulations where the primitive surface cells are repeated, the mesh is reduced to maintain a constant sampling density.

The EA of a semiconductor is the difference in energy between the conduction-band minimum in bulk material and the vacuum level. We have adopted standard practice[23,48–50] of calculating the electrostatic potential as a function of position through the slab into the vacuum, and aligning this to the corresponding potential variation in bulk diamond. For best agreement with experiment, it is normal practice to determine the offset between the bulk valence-band top and the vacuum level, and locate the conduction-band minimum using the experimental value of the band gap, 5.47 eV.

The adsorption energy per adsorbate atom corresponding to each equilibrium structure is calculated[30] as

$$E_{\text{ads}} = \frac{1}{n}\left(E_{\text{tot}} - E_{\text{surface}} - n\mu_X\right), \tag{2}$$

where E_{tot} is the total energy of the slab geometry terminated by n adsorbate atoms, E_{surface} is the total energy of a clean reconstructed diamond surface slab, and μ_X is the energy of a free metal atom.

Due to multiplet, functional, and basis-set effects it is difficult to calculate accurate energies of free transition metal atoms using standard density-functional techniques. To mitigate such errors we calculate the energy per atom for each metal species in the corresponding bulk metal, and then add the experimental cohesive energies[51] [Cu (3.49 eV), Ni(4.44 eV), Ti (4.85 eV), and V (5.31 eV)] to obtain an estimate of the free atom energy. For thermodynamically stable metal adsorption onto the diamond surface, the adsorption energies must then be negative, assuming that the loss of metals from the surface during annealing is via evaporation into an atomic state. It is important to put the absolute adsorption energies into context. For example, one might also consider the theoretical cohesive energies of Cu (4.29 eV), Ni (5.98 eV), Ti (6.29 eV), and V (6.49 eV) as a reference.[51] Such an approach would lead to considerably higher adsorption energies, but has no effect upon the relative energies of different sites or surface coverages.

The energies obtained using Eq. (2) are the average adsorption energy per metal atom, and as such may suggest

an exothermic reaction between the diamond surface and the gas of metal atoms, even if 100% surface coverages are not possible. In order to assess the energetics of the 1 ML coverages we have therefore also simulated ∼94% coverages so that the energetics of the final atom being added to the surface may be obtained. The results of these calculations are deferred to Sec. IV. The 94% surface coverage is obtained by the removal of a single metal atom from 4 × 4 surface of the most energetically favorable 1 ML coverage structures. Since the 1 ML surface coverages involve nonequivalent surface sites, in each case we have explored the removal of either site, and selected the energy from the more stable of the two.

In addition to the submonolayer coverages, 1.5 ML metal surface coverages have also been briefly examined. A range of possible sites for a metal atom added to the equilibrium 2 × 1 1 ML structures have been examined to provide a gage the energetics of thicker surface layers. The most stable structure is taken to be able to provided the characteristic energetics for 1.5 ML coverages, which are discussed in Sec. IV.

Finally, we note that the calculated energies correspond to zero temperature free energies, and therefore neglect the impact of the temperature dependence of the internal energy and the contribution of entropy.

III. RESULTS

A. Methodology validation and identification of high symmetry sites for metal atom adsorption

Our approach has recently been validated against literature values for clean, hydrogenated, and ether-terminated diamond. EAs, structures, and adsorption energies are in good agreement with theory and experiment.[24] In addition, allowing for the impact of functional, basis sets, and surface periodicities on calculations, we briefly note that the calculated properties of Ti-terminated surfaces are in reasonable agreement with recent theoretical studies.[30] More detailed comparisons are presented in Sec. III D.

In order to put the different potential equilibrium structures into context, it is convenient to label the different, high-symmetry sites occupied by metal atoms at various surface coverages. This is done with reference to the assumption, as made in previous studies, that prior to metal atom adsorption, the 2 × 1 reconstruction[52] is retained. Then four high-symmetry sites can be labeled[30,53,54] the pedestal (P), bridge (B), hollow (H), and cave (C) sites, as shown schematically in Fig. 1.

To further assess the surface site stability, two other atomic arrangements have also been examined. Perspective views of atomic arrangements corresponding to the 1-ML coverage are shown in Fig. 2. The first configuration [Fig. 2(a)] is similar to a monohydrogenated diamond (100) surface, while the second configuration [Fig. 2(b)] can be obtained by placing adsorbates midway between P and H sites. These structures are found to be relatively high in energy for each surface coverage for all metals examined.

For the candidate metal species, our aim is to identify the equilibrium structures for adatoms, 0.25, 0.50, and 1 ML of Cu, Ni, Ti, and V on diamond (001) oriented surfaces. Particularly for low coverages, it is important to note that

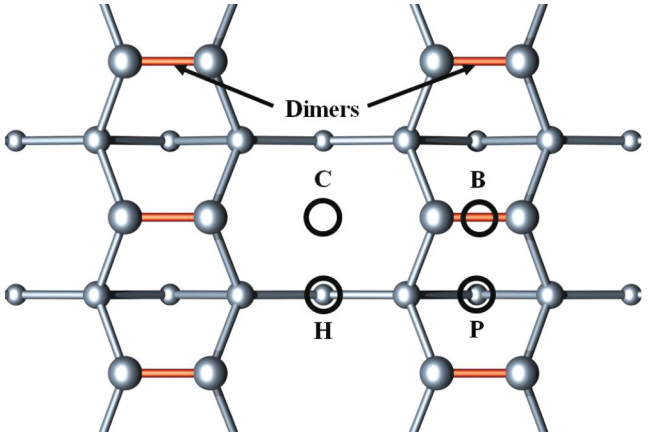

FIG. 1. (Color online) Plan view of high-symmetry adsorption sites on reconstructed C-terminated (001) (2 × 1) diamond surface. Symbols and rings indicate the sites defined in the text. The gray circles indicate the carbon atoms in the top three layers of the diamond surface, with increasing depth indicated by decreasing size.

there are many ways to achieve the same average surface atom density. For example, one adatom per four surface carbon sites corresponding to 25% might be described using reconstructed 2 × 2, 4 × 1, 4 × 2, or any number of other surface cells. We have included these three in our evaluation of the equilibrium properties of 0.25-ML coverages. For the calculations of adatom adsorption energy, a 4 × 4 supercell, made up from eight primitive 2 × 1 surface unit cells, is used to model the clean substrate. For the most stable relaxed structures for different surface coverages of the selected TM, thermodynamic stability and electronic properties are discussed in following sections.

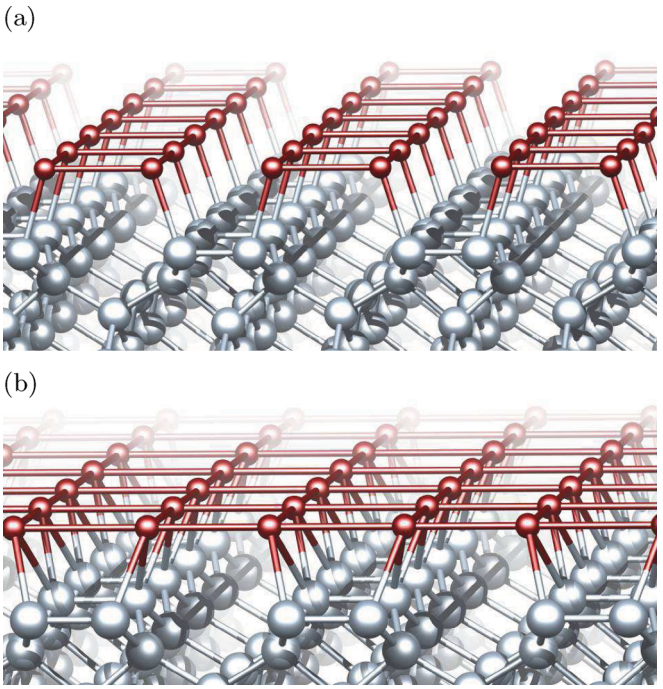

FIG. 2. (Color online) Perspective views of 1 ML of TMs on low-symmetry sites of reconstructed (001) (2 × 1) diamond surface.

TABLE I. Calculated adatom adsorption energy per adsorbate atom (E_{ads}) for Cu, Ni, Ti, and V (eV). In each case, the most stable site is indicated by the underlining.

	Site			
Metal	B	C	H	P
Ti	–	−2.85	−3.54	−5.36
V	–	−5.41	−5.60	−6.00
Ni	−2.40	−1.92	−1.84	−2.73
Cu	−1.18	−1.58	−0.95	−1.23

B. Cu termination

Copper is an attractive TM for both the CVD process and metal contact fabrication.[11,55–57] Additionally, applications such as heat sinks, where the material properties of both copper and diamond are essential[56] mean that diamond-copper interfaces are of particular interest. Since copper does not readily form a carbide, it might be expected to form a relatively abrupt and chemically inert junction with diamond.

Based upon the poor coordination strength of Cu with carbon in organometallic compounds, at low coverages of Cu the B and C sites might be expected to be favored as they have the lowest metal-carbon coordination of the four sites. In adatom calculations, we indeed find that copper favors the C site, with other sites representing metastable locations. The adatom adsorption energies are listed in Table I.

For 0.25, 0.50, and 1 ML of Cu on the diamond surface, the equilibrium structures obtained in this study are shown in Fig. 3, and the adsorption energies are summarized in Table II. Similar to adatom adsorption, the C site on 4 × 1 (0.25 ML) and 2 × 1 (0.5 ML) geometries are found to be the most stable, while the H site for all surface geometries is unstable. We also note that among the structures examined for 0.25 ML, the minimum in energy occurs where Cu atoms lie on adjacent C sites, indicating that interadsorbate interactions stabilize the adsorption of copper.

For 1 ML of Cu, a combination of B and C sites gives the most stable configuration, as shown in Fig. 3(a). Configurations including other pairings, such as P + C, P + H, and B + H, are found to be either metastable or unstable (Table II). It is also notable that Cu terminated diamond surfaces exhibit negative adsorption energies, which are increasingly stabilized with decreasing Cu coverage. This indicates that Cu-Cu interaction is helping to stabilize the surface.

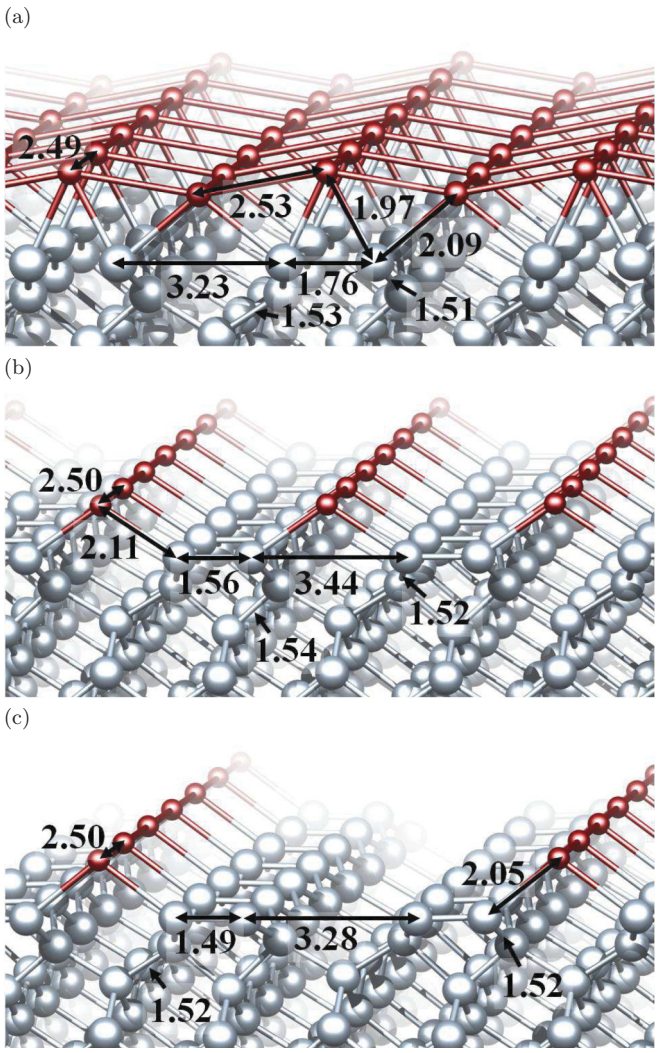

FIG. 3. (Color online) Perspective views of relaxed geometries for (a) 1.00, (b) 0.50, and (c) 0.25 ML of Cu on the (001) (2 × 1) diamond surface. Bond lengths are indicated in Å.

Depending upon the surface coverage and adsorbate sites, Cu-C bond lengths vary between 1.9 and 2.2 Å, consistent with the Cu-C bond lengths in organometalic compounds.[46]

TABLE II. Calculated adsorption energy per Cu atom, E_{ads}, EA χ, Schottky barrier, ϕ_B, dimer bond-length $d_{(C\text{-}C)}$, and carbon-copper bond length $d_{(C\text{-}Cu)}$, for varying coverages of Cu on a diamond (001) surface. Energies are in eV, lengths in Å. The B + H and P + H configurations for 1 ML, and the H site for 0.25 and 0.50 ML, are unstable.

Coverage (ML)	Site	Geometry	E_{ads}	χ	ϕ_B	$d_{(C\text{-}C)}$	$d_{(C\text{-}Cu)}$
1.00	B + C	2 × 1	−2.93	− 0.55	0.44	1.76	1.97–2.09
1.00	P + C	2 × 1	−2.83	0.05	1.04	1.73	2.08–2.23
0.50	B	2 × 1	−1.51	− 0.24	0.75	1.60	1.96
0.50	C	2 × 1	−2.51	− 0.66	0.34	1.56	2.11
0.50	P	2 × 1	−1.57	− 0.57	0.42	1.57	2.13
0.25	B	4 × 1	−1.53	− 0.31	0.68	1.37–1.58	1.95
0.25	C	4 × 1	−2.16	0.10	0.89	1.49	2.05
0.25	P	4 × 1	−1.59	− 0.13	0.86	1.37–1.57	2.12

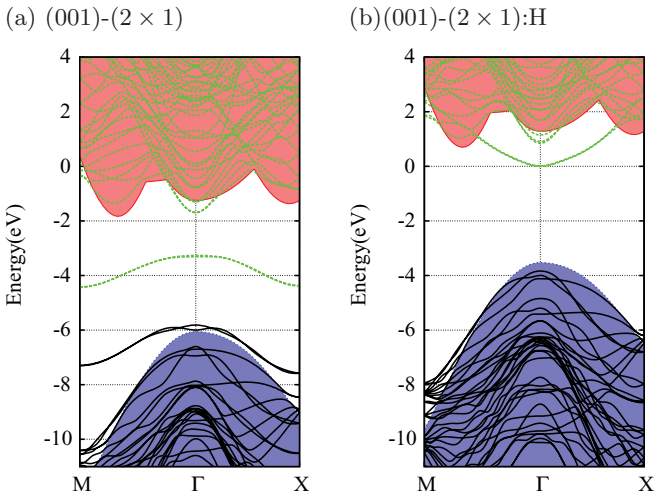

FIG. 4. (Color online) Band structures of clean and hydrogenated (001) (2 × 1) diamond surfaces. Occupied and empty bands are shown in solid (black) and dashed (green) lines, with the valence and conduction bands of the corresponding bulk diamond shown by the shading. The zero of energy is the vacuum level.

Relaxed structures (Fig. 3) retain the underlying C-C 2 × 1 reconstruction at 0.25 and 0.50 ML, but this is unstable for 1 ML. The interaction between Cu atoms has also a significant effect upon EA; the values vary between a PEA of 0.10 eV and a NEA of −0.55 eV with coverage and geometry (Table II).

To further illustrate the electronic properties as a function of coverage, we have calculated the band structures corresponding to the most stable configurations of 0.25, 0.50, and 1 ML. The band structures of C-terminated surfaces, plotted in full in Fig. 4, are superimposed upon those of the Cu-terminated surfaces in Fig. 5. States resembling those from the carbon dimers on unterminated (001) surfaces of π and π^* character lie around the top of the bulk valence band. Figure 5(a) shows that for 1 ML of Cu, several occupied and unoccupied states are present above the diamond valence band. Inspection of wave functions of the filled and empty levels suggests the partially occupied states around −4.10 eV and the empty band around −1.00 eV corresponds to d orbitals localized in the Cu layer, whereas the empty states around −1.80 eV are due to hybridized orbitals related to both C and Cu atoms.

There are fewer bands in the diamond gap for partial surface coverages, and they are less dispersive. In case of 0.50 ML, partially occupied states near −5.90 eV mainly originated from a strong antibonding combination of surface Cu d orbitals with the host π^*-like states, while the fully unoccupied states around −2.30 eV are the results of bonding combination of surface π and Cu d orbitals. For 0.25 ML, pairs of electronic states near −4.50 and −2.00 eV are similar to 0.50 ML, and formed from bonding and antibonding of Cu d orbitals with the host surface reconstructions.

C. Ni termination

Previous studies of the Ni-diamond interface[12,31] indicates that Ni adsorption may lead to a NEA. Photoemission spectra confirm a sharp NEA peak,[12] however the magnitude of NEA is not known. Despite the low thermodynamic stability of nickel carbide, we find, based upon the adsorption energy in Table III, that Ni shows a strong adhesion with the diamond surface. In contrast to Cu, adatom adsorption of Ni favors the P site (Table I), being 0.33 eV more stable than the B site.

The stability of the P site is reduced with increasing coverage, where B and C sites are favored (Table III). In common with Cu, the B + C configuration is found to be the most energetically favorable arrangement for 1 ML of Ni. Furthermore, at 0.25-ML coverage, for every high-symmetry site, adsorption of Ni on 4 × 1 geometry (where surface adsorption sites are adjacent) is more stable than that on 2 × 2 and 4 × 2 geometries, again indicating the energetic favorability of structures with metals on adjoining sites.

We find that an underlying 2 × 1 reconstruction in the uppermost carbon layer is unstable for 1 ML of Ni. However, as with Cu, for Ni this 2 × 1 reconstruction is preserved at these lower coverages. The C-Ni bond lengths lie in the 1.82–2.12 Å range, close to the C-Ni bond lengths[46] in organometallic compounds (∼1.90 Å). The adsorption energies, listed in Table III, show that the formation of a metal layer from Ni is more energetically favorable than the corresponding reaction with Cu. Experimentally, it is known[11] that Cu has a tendency to form islands. The relatively stronger interaction between Ni and diamond found here may suggest that island formation will be less prevalent in this case.

Akin to Cu adsorption on 2 × 1 and 4 × 1 geometries, Ni-Ni interactions appear to have an impact upon EAs. At 0.25 ML we find a small PEA, whereas at 0.50 and 1 ML we obtain NEAs of −0.78 and −0.29 eV, respectively. The relatively higher stability, and the very small barrier height of nickel on diamond relative to Cu makes it more favorable for the formation of ohmic contacts, critical in the development of low-resistance metal-diamond interfaces for diamond electronics.

The band structures corresponding to different coverages of Ni are shown alongside those of Cu termination. Similar to Cu termination, as shown in Fig. 5, several bands are present in the band gap of the underlying clean diamond. In all cases, states in the band gap of the underlying diamond are linear combinations of Ni 3d orbitals, and in the cases of partial coverage, π and π^* states from the underlying surface reconstructions.

D. Ti termination

Consistent with its carbide-forming nature, Ti experimentally exhibits strong adhesion with the diamond surface, able to withstand the high temperatures, and is compatible with conventional diamond growth and device processing techniques.[1,58] Additionally, the growth rate on carbide-forming substrates is higher than on substrates that do not form a carbide.[58] Strong adhesion at the metal-diamond interface may reasonably be expected to affect the electronic and structural properties significantly. In our simulations, adsorption energies for all surface coverages of Ti are more favorable than those found for Cu and Ni (Table IV).

For Ti adatom adsorption, the P site exhibits a highly exothermic adsorption of 5.36 eV per Ti atom (Table I). On increasing the surface coverage to 0.25 ML, the P site becomes relatively less stable, and Ti atoms marginally prefer H sites. We note that this result shows a small quantitative deviation

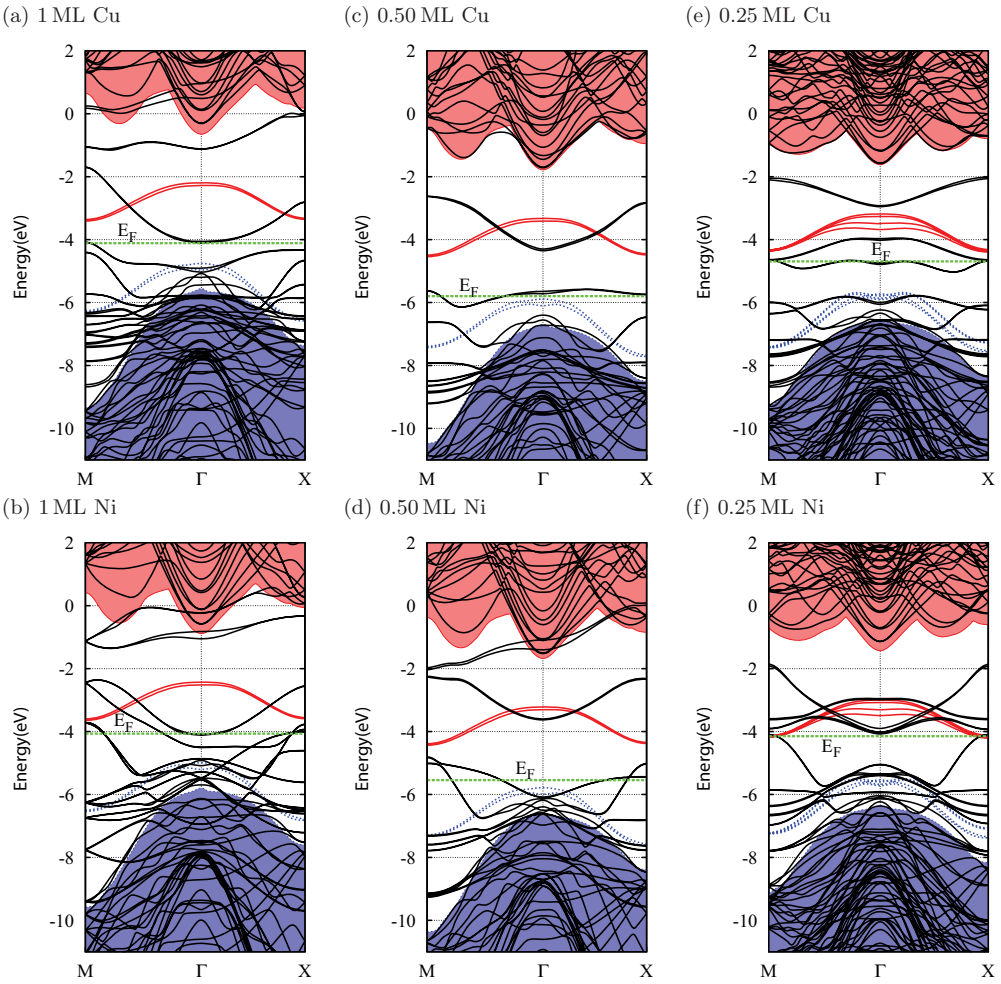

FIG. 5. (Color online) Band structures in the vicinity of the band gap along high-symmetry directions in the Brillouin zone for various coverages of Cu and Ni on (001) diamond surfaces. Black lines represent the states of the metal-terminated surfaces with the occupancy indicated by the location of the Fermi level. Blue and red lines correspond to occupied and empty states of the C-terminated surface [Fig. 4(a)]. The zero of the energy scale is the vacuum level, and the C-terminated surface band structure is aligned such that the average potential in the bulk of the slab is coincident with the same region in the metal-terminated cases.

with previous calculations[30] of Ti terminated diamond surfaces which suggested a P site for this coverage. This difference may arise from the periodicity of the surface cell, as the most stable, 4×2 surface geometry for a 0.25 ML coverage was

TABLE III. Calculated adsorption energy per Ni atom, E_{ads}, EA χ, Schottky barrier, ϕ_B, dimer bond length $d_{(C-C)}$ and carbon-nickel bond length $d_{(C\text{-}Ni)}$, for varying coverages of Ni on a diamond (001) surface. Energies are in eV, lengths in Å. The P + C configuration for 1 ML is unstable.

Coverage (ML)	Site	Geometry	E_{ads}	χ	ϕ_B	$d_{(C\text{-}C)}$	$d_{(C\text{-}Ni)}$
1.00	B + C	2×1	−4.25	− 0.29	0.15	2.50	1.85
1.00	B + H	2×1	−4.10	0.20	0.63	2.54	1.82–2.07
1.00	P + H	2×1	−3.60	0.67	1.1	2.50	2.06
0.50	B	2×1	−3.12	− 0.56	− 0.13	1.51	1.87
0.50	C	2×1	−3.34	− 0.78	− 0.33	1.96	1.92
0.50	H	2×1	−2.91	0.70	1.13	1.70	2.12
0.50	P	2×1	−2.98	0.13	0.56	1.50	2.07
0.25	B	4×1	−3.18	− 0.26	0.17	1.37–1.50	1.88
0.25	C	4×1	−3.06	0.28	0.71	1.49	1.99
0.25	H	4×1	−2.38	0.50	0.93	1.53	2.01
0.25	P	4×1	−2.99	0.30	0.73	1.37–1.50	2.07

TABLE IV. Calculated adsorption energy per Ti atom, E_{ads}, EA χ, Schottky barrier, ϕ_B, dimer bond length $d_{(C\text{-}C)}$, and carbon-titanium bond length $d_{(C\text{-}Ti)}$, for varying coverages of Ti on a diamond (001) surface. Energies are in eV, lengths in Å. The P + C configuration for 1 ML is unstable.

Coverage (ML)	Site	Geometry	E_{ads}	χ	ϕ_B	$d_{(C\text{-}C)}$	$d_{(C\text{-}Ti)}$
1.00	B + C	2 × 1	−4.60	− 0.29	0.85	1.61	2.22
1.00	B + H	2 × 1	−5.08	0.35	1.51	1.65	2.19–2.32
1.00	P + H	2 × 1	−4.72	1.56	2.70	2.49	2.25
0.50	B	2 × 1	−3.66	− 2.00	− 0.86	1.79	1.98
0.50	C	2 × 1	−3.91	− 2.05	− 0.91	1.66	2.12
0.50	H	2 × 1	−5.02	0.21	1.35	1.65	1.97–2.26
0.50	P	2 × 1	−3.77	0.52	1.66	1.73	2.14
0.25	B	4 × 1	−3.86	− 1.52	− 0.38	1.38–1.74	1.99
0.25	C	4 × 1	−3.33	− 0.72	0.42	1.51	2.17
0.25	H	4 × 2	−4.71	− 0.90	0.25	1.62	2.04–2.19
0.25	P	2 × 2	−4.69	− 3.64	− 2.50	1.64	2.03

not reported previously; we find that for 0.25 ML of Ti, the H site on 4 × 2 geometry is just 0.10 eV/atom higher in energy than the P site on 2 × 2 geometry. The calculated adsorption energies for the P site on 4 × 2 geometry and the H site on 2 × 2 are found to be virtually indistinguishable at −4.69 and −4.65 eV/atom, respectively.

Our calculations for 0.50 ML coverage are qualitatively in agreement with previous calculations,[30] which also found the H site as the most energetically favorable location. By considering the difference between experimental and theoretical cohesive energies (1.44 eV) and the effect of functional and basis sets, one can compare the calculated adsorption energies with those reported.[30] Using LDA cohesive energies for the most stable configurations, adatom, 25%, and 50% coverages are calculated here to be 6.80, 6.13, and 6.46 eV, respectively, which agree well with the previously calculated adsorption energies[30] of 7.19, 6.62, and 6.85 eV, respectively.

For 1 ML of Ti, a combination of B + H sites is most stable, with the equilibrium geometry shown schematically in Fig. 6. The P + C combination is unstable, spontaneously reconstructing to B + H. It is worth noting that the H site is favored quite generally for Ti termination, (Fig. 6). Based upon internuclear distances, relaxed structures indicate the formation of four strong Ti-C covalent bonds at this site.

The calculated single and dimer C-C bond lengths for 2 × 1 (100) clean and H-terminated diamond surfaces are found to be 1.61 and 1.37 Å, respectively.[24] Here we use them as the criterion to compare the surface C-C bond lengths of metal-terminated surfaces. For the most stable surface sites, even at high Ti coverages (Fig. 6), the 2 × 1 C-C reconstruction is retained. The C-C bond-length of 1.65 Å is around 20% greater than the dimer bond length of the clean surface, but just 2.5% greater than the H-terminated surface, indicating that the reconstruction is a single C-C bond, allowing for covalent bonding between the surface C sites and the Ti adsorbates. Calculated surface C-Ti bond lengths (∼2.15 Å) are consistent with C-Ti bond lengths (2.17 Å) in organometallic compounds.[46]

We now consider the electronic and electrical properties. The calculated EA increases with increasing Ti coverage. For a 0.25 ML, an NEA of −0.90 eV is found. For the low-energy P site, the NEA is very large at −3.64 eV, a

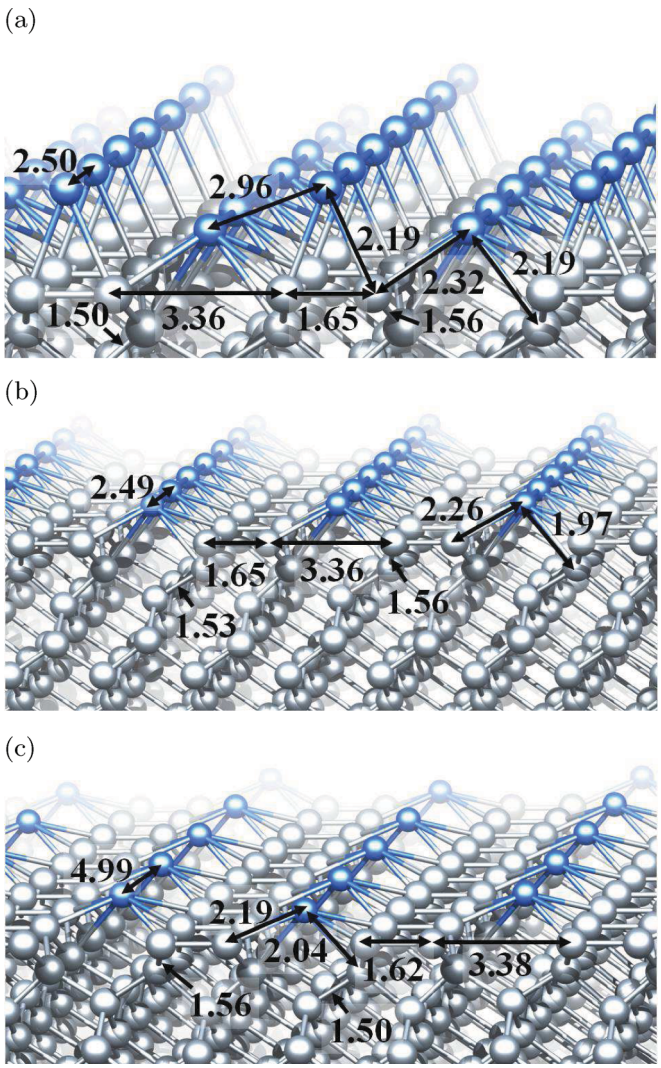

FIG. 6. (Color online) Perspective views of relaxed geometries for (a) 1.00, (b) 0.50, and (c) 0.25 ML of Ti on the (001) (2 × 1) diamond surface. Bond lengths are indicated in Å.

TABLE V. Calculated adsorption energy per V atom, E_{ads}, EA χ, Schottky barrier, ϕ_B, dimer bond length $d_{(C\text{-}C)}$, and carbon-vanadium bond length $d_{(C\text{-}V)}$, for varying coverages of V on a diamond (001) surface. Energies are in eV, lengths in Å. The P + C configuration for 1 ML and the P site for 0.50 ML are unstable.

Coverage (ML)	Site	Geometry	E_{ads}	χ	ϕ_B	$d_{(C\text{-}C)}$	$d_{(C\text{-}V)}$
1.00	B + C	2 × 1	−5.99	− 0.38	0.79	2.50	2.16
1.00	B + H	2 × 1	−6.45	− 0.03	1.14	1.69	2.22–2.45
1.00	P + H	2 × 1	−6.22	0.86	2.04	1.71	2.38–2.45
0.50	B	2 × 1	−5.25	− 1.66	− 0.49	1.68	2.04
0.50	C	2 × 1	−6.06	− 1.55	− 0.38	1.60	2.17
0.50	H	2 × 1	−6.60	− 0.76	0.41	1.68	2.30
0.25	B	4 × 1	−5.33	− 1.15	0.02	1.37–1.66	2.04
0.25	C	2 × 2	−5.80	− 0.95	0.22	1.58	2.14
0.25	H	4 × 1	−6.10	0.02	1.20	1.52	2.34
0.25	P	4 × 1	−5.87	− 0.43	0.74	1.37–1.64	2.17

consequence of this structure giving rise to simultaneously large charge transfer between the adsorbate and the surface, and a large geometric separation of the charges. The tendency towards a PEA with increasing coverage reflects the impact of the direct interaction between neighboring Ti atoms on the surface.

The band structure of the most stable configurations are shown in Fig. 7. We observe that in comparison to 1 ML of Cu or Ni, a large number of highly dispersed states are present. The electronic states in the energy range from −2.00 to −5.00 eV are mainly *d* orbitals, localized within the surface Ti layer.

For both 0.50 and 0.25 ML of Ti [Figs. 7(c) and 7(e)], the band structures show surface bands, which we find to have significant 3*d* character. The electronic states in the middle of bulk band gap are either due to essentially Ti-related *d* orbitals, or to an antibonding combination of these orbitals with surface π^*-like states. As an interesting feature, the electronic band structure corresponding to 0.25 ML [Fig. 7(e)] shows a small band gap of around 0.7 eV along the M-Γ-X branches.

E. V termination

The vanadium/diamond interfacial structures have received relatively very little attention to date. However, vanadium-carbon bond functionalities on the diamond surface, and particularly on nanodiamond, have the potential for use in metal-induced stoichiometric and catalytic transformations.[59,60] Vanadium readily forms a carbide and is therefore expected to behave in a fashion closer to Ti than to Cu or Ni.

In line with Ti adatom adsorption, the P site is the most energetically favorable for a V adatom (Table I), followed by the H site. Both P and H sites exhibit exothermic reactions relative to a clean diamond surface and vanadium metal in addition to being highly exothermic with respect to free V atoms.

For partial surface coverage of V, the H site on 4 × 1 and 2 × 1 is found to be the most energetically favorable, consistent with the view that interadsorbate interactions are energetically favored (Table V). Similar to Ti, the combination of sites B and H gives the most stable arrangement for 1 ML adsorption. It is important to note here that for 0.50 ML, the P site is completely unstable: in the absence of an artificial symmetry constraint, in our simulations all V atoms initially located at P sites move spontaneously to H sites.

Unlike Ti termination, the C-C reconstruction is lost for 1 ML, while it is retained at partial surface coverages. The measured C-V bond lengths are in the 2.04–2.45 Å range (Table V), close to the value of 2.11 Å found in organometallic systems.[46] The adsorption energy increases from around −6.0 eV for an individual adatom, to around −6.5 eV/atom for the complete monolayer, consistent with the formation of chemically stable C-V covalent interactions.

As already described for Cu, Ni, and Ti, the interaction between vanadium atoms has also a significant impact upon the EA. Due to the complex interplay between vanadium-carbon and vanadium-vanadium interactions, both in terms of charge exchange and geometry, surfaces with 1 ML of V exhibit a small NEA, whereas at 0.50 ML V coverage, a large NEAs of −0.76 eV is determined.

The band structures (Fig. 7) corresponding to the most stable structures are found to be qualitatively similar those of Ti.

IV. DISCUSSION AND CONCLUSION

We have performed density-functional simulations for four TMs absorbed on a 2 × 1 reconstructed (001) diamond surfaces. Based upon the metal-diamond chemical interactions, there is a clear divide. For Ti and V, which form carbides, the metal atoms interact strongly with the surface carbon atoms, while Cu and Ni, which do not readily form carbides, exhibit relatively weaker interactions. As a consequence of the C-metal interactions, the surface reconstructions are strongly affected by the adsorbates and at a high surface coverage (1 ML) of Cu and Ni, the underlying C-C reconstructed bonds are unstable, whereas for all surface coverage of Ti, the C-C reconstruction is retained. Relaxed geometries also indicate that metal atoms interact strongly with each other. In the case of non-carbide-forming TMs, metal-metal interactions appear more significant than the carbide-forming metals.

The chemical nature of the metal and surface coverages have a qualitative impact upon both the energies of adsorption and EA. From the calculated adsorption energies of Cu, Ni, Ti, and V, it can be concluded that diamond surface treatment with carbide-forming metals, as evidenced by Ti and V, would yield a more thermodynamically stable termination in comparison to non-carbide-forming metals.

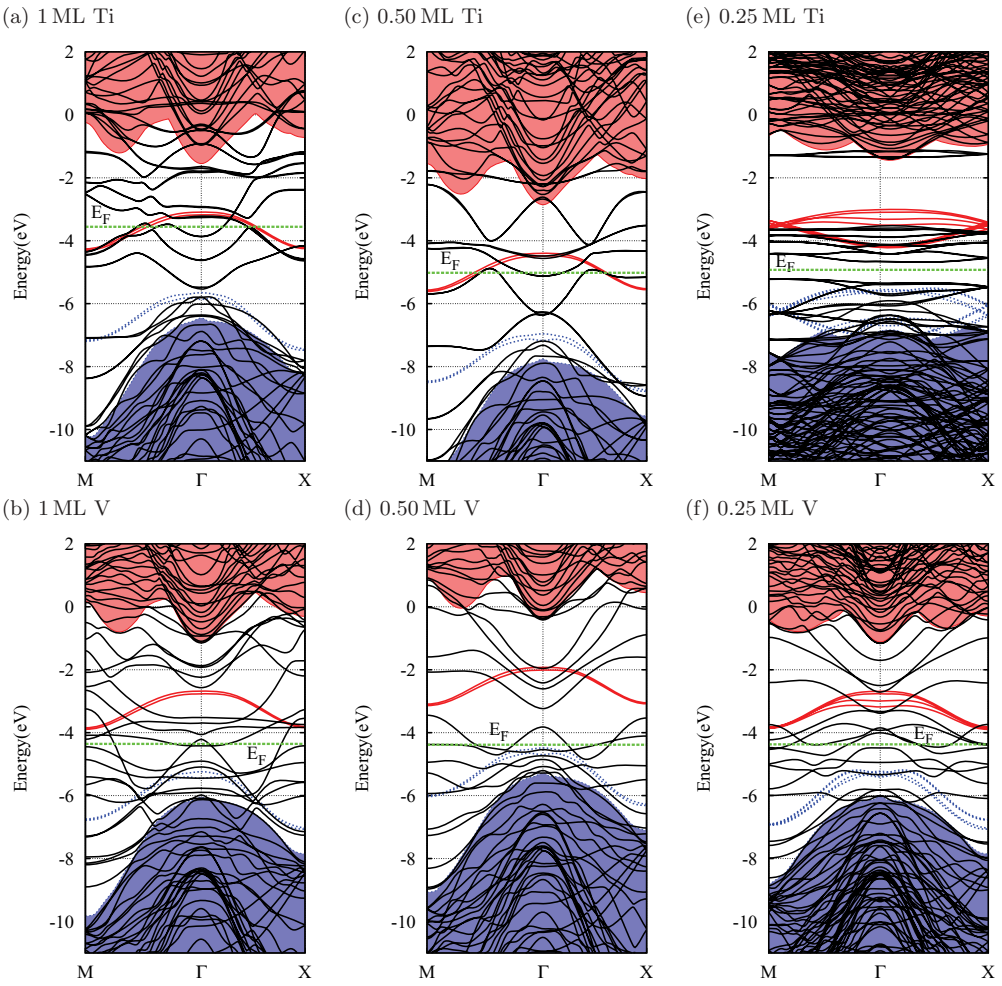

FIG. 7. (Color online) Band structures in the vicinity of the band gap along high-symmetry directions in the Brillouin zone for various coverages of Ti and V on (001) diamond surfaces. Lines, shading, and alignment are as in Fig. 5.

The *absolute* magnitude of the adsorption energy deserves further discussion. The main source of variance arising between differing calculations and experiment is likely to be the way in which the energy of the metal atoms are taken into account. In this study, in line with common practice in this field, we have taken the reference state to be that of a free metal atom. As noted in the introduction, there is some difficulty in obtaining accurate values for the energies of free atoms due to a number of computational and quantum-mechanically based issues. If we take as an example the cases of the carbide-forming species, we find that the cohesive energies of V and Ti differ by 0.20 eV according to theory, and 0.46 eV in experiment. More significantly, the difference between the theoretical and experimental cohesive energies of V, Ti, Ni, and Cu are 1.18, 1.44, 1.54, and 0.80 eV/atom. Using the theoretical of the energies per atom will therefore, on average, lead to an overestimate in the adsorption energy of more than 1 eV, and when comparing absolute energies between models, the uncertainty in the value of the reference state of the adsorbate must be considered with great care.

Nevertheless, the very large adsorption energies obtained relative to free atoms whether referenced to calculated or experimental data reflect a process whereby individual metal atoms leave the surface only at high temperatures. As a consequence of the large adsorption energies one can conclude that, at least in the cases of the metal species analyzed in this paper, the adsorbates would persist on the diamond surface to relatively high temperatures prior to the desorption of individual atoms into a vapor.

The calculations performed for 94% surface coverage described in Sec. II show that the average adsorption energies corresponding to 1-ML surface coverage are very close in magnitude, but slightly higher than those of 94%. The slight increase in average adsorption energy corresponding to the addition of the final metal atom on a 16-site surface means that the heat of reaction of final metal atom is exothermic, and hence it is thermodynamically favorable to form a complete ML of the TMs investigated in this study. Indeed, the increasing magnitude of average adsorption energy from 94 to 100% coverage suggests that the reaction energy for the final metal atom is *greater* than the average energy of the preceding ones. This can be understood as being a consequence of the increasing degree to which the metal adsorbates are able to form inter-TM bonds, in addition to the termination of the diamond surface.

However, these conclusions must be treated with care. It is possible, if not likely, that some metal species would be prone to migration over the surface at a temperature below

that required for desorption. If this can happen, either during deposition or subsequent annealing, then the metal atoms may migrate to form islands on the surface rather than desorb. The likelihood of this can be considered in a thermodynamic sense by examining the adsorption energies relative to the native elemental state of each TM adsorbate species. In the cases of both Cu and Ni, at all coverages the adsorption energy is *positive* relative to the metals in the bulk metal state, so that for these species, at low coverage, island formation tends to be energetically favored. In contrast, for Ti and V, for the most stable structure at each coverage the adsorption energy remains less than or equal to zero, even when referenced to the bulk metals, so that the aggregation into islands is less energetically favored.

Although a full analysis of the energetics for the formation of thicker than 1-ML layers is beyond the scope of this paper for reasons outlined in Sec. II, some quantitative data has been produced by simulation of 1.5-ML surface coverages, where the strain introduced by the formation of the metal solid layer is likely to be less significant than for multiple, full ML coverages. Our preliminary calculations show that for Cu and Ni, a higher adsorption energy is obtained in comparison to those of 1 ML, while for Ti and V the adsorption energies are somewhat smaller. This further supports the view that for non-carbide-forming TMs, such as Cu and Ni, due to the relative strengths of the metal-carbon and metal-metal interaction, energetics favor island formation, whereas for carbide-forming materials, such as Ti and V, which are strongly bound to the diamond surface, the energetics favor complete ML formation. The question of surface migration of TMs over the diamond surface remains to be addressed.

Of the species examined, the carbide-forming TMs exhibit large and negative EAs at low coverages, while non-carbide-forming species tend to yield an NEA at high surface coverages. In addition to the chemical nature and surface coverage, the EA is also sensitive to the adsorption site. For example, the H and P sites at 0.50-ML surface coverage of Ti give PEAs that differ by 0.4 eV. Even more significant is that at 0.25 ML of Ti, the B and P sites give large NEAs, which differ by more than 2 eV due to a combination of charge transfer and geometric factors.

Overall, our calculations suggest that it is possible to produce surface treatments that yield a large NEA on diamond by depositing a submonolayer coverage of TMs. However, selective deposition of submonolayer coverages of TMs is likely to be technologically challenging. The use of atomic layer deposition and scanning-probe-based lithography for atomic-scale patterning of TMs on diamond surface,[61,62] may offer a potential solution in the laboratory.

In the band structures of TMs, at higher surface coverages, most of the electronic states in the band gap are associated with either localized 3*d* orbitals centered on metal atoms or with a set of states reflecting the bonding interactions between C and metal atoms made up from with sp^n hybrids and *d* orbitals. An underlying carbon-dimer character is generally visible in terms of π-related deep bands only at partial surface coverages, where there are wave functions with π^* character.

The calculated Schottky barrier heights calculated for ultrathin, 1 ML of Cu, Ni, and Ti are and 0.44, 0.63, and 1.51 eV, respectively, may be compared with the experimental Schottky barrier heights for few-layer-thick TMs, which are respectively 0.70, 0.70, and 1.20 eV.[10–13] The agreement between theory and experiment is viewed as very reasonable, and the small differences can be attributed to combinations of the true metal thickness, photovoltaic effects in measurements and the presence of interfacial impurities, such hydrogen and particularly oxygen. The measured Schottky barrier height for Ni in this study shows a quantitative difference with the Schottky barrier height of 0 eV, calculated previously,[31] but in the previous study their results are based on ideal, unrelaxed structures. Although very little theoretical or experimental data is available for vanadium-diamond interfaces, a key conclusion can be derived from this study that from the thermal stability and EA perspectives, TMs, particularly, carbide-forming TMs have great potential for both NEA devices and chemical functionalization applications.

ACKNOWLEDGMENTS

We thank Dr. Ulrich Baisch for providing his help with the structure of vanadium carbide (VC). This work is supported by BAE Systems and the Engineering and Physical Sciences Research Council (EPSRC) UK through the DHPA scheme.

[1] T. Tachibana, B. E. Williams, and J. T. Glass, Phys. Rev. B **45**, 11968 (1992).
[2] T. Teraji, S. Koizumi, and Y. Koide, J. Appl. Phys. **104**, 016104 (2008).
[3] K. Das, V. Venkatesan, K. Miyata, D. L. Dreifus, and J. T. Glass, Thin Solid Films **212**, 19 (1992).
[4] J. W. Glesener, A. A. Morrish, and K. A. Snail, J. Appl. Phys. **70**, 5144 (1991).
[5] A. T. Collins, Semicond. Sci. Technol. **4**, 605 (1989).
[6] P. W. May, Philos. Trans. R. Soc. A **358**, 473 (2000).
[7] *Diamond Films and Coatings: Development, Properties and Applications*, edited by Robert F. Davis (William Andrew Publishing, New York, 1994).
[8] R. L. Bell, in *Negative Electron Affinity Device* (Clarendon Press, Oxford, 1973).
[9] M. W. Geis, J. C. Twichell, and T. M. Lyszczarz, J. Vac. Sci. Technol. B **14**, 2060 (1996).
[10] P. K. Baumann and R. J. Nemanich, J. Appl. Phys. **83**, 2072 (1998).
[11] P. K. Baumann and R. J. Nemanich, Phys. Rev. B **58**, 1643 (1998).
[12] J. van der Weide and R. J. Nemanich, Phys. Rev. B **49**, 13629 (1994).
[13] J. van der Weide and R. J. Nemanich, J. Vac. Sci. Technol. B **10**, 1940 (1992).
[14] M. W. Geis, N. N. Efremow, J. D. Woodhouse, M. D. McAleese, M. Marchywka, D. G. Socker, and J. F. Hochedez, IEEE Electron Device Lett. **12**, 456 (1991).

[15]M. Suzuki, T. Ono, N. Sakuma, and T. Sakai, Diamond Relat. Mater. **18**, 1274 (2009).
[16]F. A. M. Koeck and R. J. Nemanich, Diamond Relat. Mater. **15**, 217 (2006).
[17]L. J. Brillson, Surf. Sci. Rep. **2**, 123 (1982).
[18]S. B. Zhang, M. L. Cohen, and S. G. Louie, Phys. Rev. B **32**, 3955 (1985).
[19]S. Kurtin, T. C. McGill, and C. A. Mead, Phys. Rev. Lett. **22**, 1433 (1969).
[20]J. Tersoff, Phys. Rev. B **30**, 4874 (1984).
[21]S. M. Sze and K. K. Ng, *Physics of Semiconductor Devices*, 3rd ed. (Wiley, Hoboken, 2006).
[22]E. H. Rhoderick and R. H. Williams, in *Metal-Semiconductor Contacts* (Clarendon Press, Oxford, 1988).
[23]S. J. Sque, R. Jones, and P. R. Briddon, Phys. Rev. B **73**, 085313 (2006).
[24]A. K. Tiwari, J. P. Goss, P. R. Briddon, N. G. Wright, A. B. Horsfall, R. Jones, H. Pinto, and M. J. Rayson, Phys. Rev. B **84**, 245305 (2011).
[25]F. Maier, J. Ristein, and L. Ley, Phys. Rev. B **64**, 165411 (2001).
[26]K. W. Wong, Y. M. Wang, S. T. Lee, and R. W. M. Kwok, Diamond Relat. Mater. **8**, 1885 (1999).
[27]R. S. Balmer, J. R. Brandon, S. L. Clewes, H. K. Dhillon, J. M. Dodson, I. Friel, P. N. Inglis, T. D. Madgwick, M. L. Markham, T. P. Mollart, N. Perkins, G. A. Scarsbrook, D. J. Twitchen, A. J. Whitehead, J. J. Wilman, and S. M. Woollard, J. Phys.: Condens. Matter **21**, 364221 (2009).
[28]L. Diederich, O. M. Küttel, P. Aebi, E. Maillard-Schaller, R. Fasel, and L. Schlapbach, Diamond Relat. Mater. **7**, 660 (1998).
[29]M. W. Geis, J. C. Twichell, J. Macaulay, and K. Okano, Appl. Phys. Lett. **67**, 1328 (1995).
[30]Y. Jia, W. Zhu, E. G. Wang, Y. Huo, and Z. Zhang, Phys. Rev. Lett. **94**, 086101 (2005).
[31]W. E. Pickett and S. C. Erwin, Phys. Rev. B **41**, 9756 (1990).
[32]H. Guo, Y. Qi, and X. Li, J. Appl. Phys. **107**, 033722 (2010).
[33]J. P. Perdew and Y. Wang, Phys. Rev. B **45**, 13244 (1992).
[34]P. R. Briddon and R. Jones, Phys. Status Solidi B **217**, 131 (2000).
[35]M. J. Rayson and P. R. Briddon, Comput. Phys. Commun. **178**, 128 (2008).
[36]C. Hartwigsen, S. Goedecker, and J. Hutter, Phys. Rev. B **58**, 3641 (1998).
[37]J. P. Goss, M. J. Shaw, and P. R. Briddon, in *Theory of Defects in Semiconductors*, Vol. 104 of Topics in Applied Physics, edited by David A. Drabold and Stefan K. Estreicher (Springer, Berlin, 2007), pp. 69–94.
[38]M. J. Rayson and P. R. Briddon, Phys. Rev. B **80**, 205104 (2009).
[39]J. Singh, *Physics of Semiconductors and Their Heterostructures* (McGraw-Hill, New York, 1993).
[40]D. A. Liberman, Phys. Rev. B **62**, 6851 (2000).
[41]M. J. Mehl and D. A. Papaconstantopoulos, Phys. Rev. B **54**, 4519 (1996).
[42]A. Aguayo, G. Murrieta, and R. de Coss, Phys. Rev. B **65**, 092106 (2002).
[43]M. Binnewies and E. Milke, *Thermochemical Data of Elements and Compounds* (Wiley, New York, 1999).
[44]R. G. Coltters, Mater. Sci. Eng. **76**, 1 (1985).
[45]*Handbook of Chemistry and Physics*, edited by D. R. Lide, Vol. 87 (CRC Press, Boca Raton, Florida, 2006).
[46]*Handbook of Chemistry and Physics*, edited by David R. Lide, Vol. 87 (CRC Press, Boca Raton, Florida 2006), pp. 17–18.
[47]H. J. Monkhorst and J. D. Pack, Phys. Rev. B **13**, 5188 (1976).
[48]M. J. Rutter and J. Robertson, Phys. Rev. B **57**, 9241 (1998).
[49]C. J. Fall, N. Bingeli, and A. Baldereschi, J. Phys.: Condens. Matter **11**, 2689 (1999).
[50]G. Kern and J. Hafner, Phys. Rev. B **56**, 4203 (1997).
[51]P. H. T. Philipsen and E. J. Baerends, Phys. Rev. B **54**, 5326 (1996).
[52]P. Krüger and J. Pollmann, Phys. Rev. Lett. **74**, 1155 (1995).
[53]Y. Morikawa, K. Kobayashi, and K. Terakura, Surface Sci. **283**, 377 (1993).
[54]T. Abukawa and S. Kono, Phys. Rev. B **37**, 9097 (1988).
[55]M. Sommer, R. Haubner, and B. Lux, Diamond Relat. Mater. **9**, 351 (2000).
[56]Z.-B. Ma, Q.-C. Wu, X.-S. Shu, J.-H. Wang, C.-X. Wang, and X.-F. Li, Plasma Sci. Tech. **2**, 207 (2000).
[57]X. G. Wang and J. R. Smith, Phys. Rev. Lett. **87**, 186103 (2001).
[58]B. V. Spitsyn, L. L. Bouilov, and B. V. Derjaguin, J. Cryst. Growth **52**, 219 (1981).
[59]J. M. Rosset, C. Floriani, M. Mazzanti, A. Chiesi-Villa, and C. Guastini, Inorg. Chem. **29**, 3991 (1990).
[60]G. P. Bogatyreva, M. A. Marinich, E. V. Ishchenko, V. L. Gvyazdovskaya, G. A. Bazalii, and N. A. Oleinik, Phys. Solid State **46**, 738 (2004).
[61]J. R. Tucker, C. Wang, and T.-C. Shen, Nanotechnol. **7**, 275 (1996).
[62]T.-C. Shen, C. Wang, J. W. Lyding, and J. R. Tucker, Appl. Phys. Lett. **66**, 976 (1995).